J Mater Sci (2007) 42:4757–4762
DOI 10.1007/s10853-006-0890-1

α Transition of polyamide 6 in chemically bonded polyamide 6/polytetrafluoroethylene compounds studied by dynamic mechanical thermal analysis and dielectric thermal analysis

Jun Zhao

Received: 6 February 2006 / Accepted: 24 August 2006 / Published online: 19 March 2007

Abstract The α transition of polyamide 6 (PA 6) component in chemically bonded PA 6/polytetrafluoroethylene (PTFE) compounds is studied by dynamic mechanical thermal analysis (DMTA) and dielectric thermal analysis (DETA). It is found that DMTA shows better compatibility between two components than DETA does. It is also found that at the α transition temperature of PA 6 component ($T_{\alpha}^{PA\,6}$), the dynamic mechanical response of PTFE component is remarkable while its dielectric response is negligible. The effect of PTFE component on the segmental mobility of PA 6 component is discussed on the basis of DMTA, DETA and differential scanning calorimetry (DSC) results and the chemical bonding effect is found to play the dominant role. The measurement of apparent activation energy (ΔE_a) shows that the addition of PTFE component reduces the cooperativity of the α transition of PA 6 component.

Introduction

Polyamide (PA)/polytetrafluoroethylene (PTFE) compounds produced by reactive extrusion possess very low coefficient of sliding friction and low wear rate promoting their use in maintenance-free sliding bearings [1]. The basis of these novel properties is the formation of chemical bonds between PA and PTFE components by transamidation in a melt modification reaction. So the effective processing and the material properties of PA component can be combined with the excellent anti-friction properties of PTFE component in these materials [2]. Lehmann et al. pointed out that the formation of chemically bonded PA/PTFE compounds was based on the following three points [2]. First of all, PTFE modified with carboxylic acid groups could be produced by electron beam irradiation of commercial PTFE micropowders in the presence of oxygen, and then the generated carbonyl fluoride groups transferred into carboxylic acid groups by hydrolysis post-treatment. Secondly, carboxylic acid groups were found to exhibit a very high reactivity under PA melt conditions [3]. The last but not the least important, melt mixing devices like compounders or twin screw extruders with high shear rates were employed to obtain a good distribution and a further break down of the PTFE micropowders with a size of ca. 2–8 μm in the PA melt matrix. It was due to these three points that graft and block copolymers could be produced in a melt modification reaction by reactive extrusion. In their further work, the dispersity of PTFE phase and the efficiency of the in-situ reaction have been characterized by various techniques, such as differential scanning calorimetry (DSC), atomic force microscopy (AFM), scanning electron microscopy (SEM), dynamic light scattering (DLS), Fourier transform infrared (FTIR) spectroscopy, and the notched impact strength measurements [4–6]. However, comprehensive understanding of the structure–property relationships is still needed to further commercialize these new PA/PTFE materials.

Both dynamic mechanical thermal analysis (DMTA) and dielectric thermal analysis (DETA) are sensitive to the local environment surrounding molecules and have been widely used as probes for the molecular dynamics of polymers [7–11]. Between them, DMTA is sensitive to the fluctuations of internal stresses while DETA sensitive to

J. Zhao (✉)
Max Planck Institute for Polymer Research, Ackermannweg 10, 55128 Mainz, Germany
e-mail: junzhao1974@hotmail.com

the fluctuations of dipole moments. Therefore, a comparison between them can give deeper insight into the molecular processes [9, 10]. In Song's work, the compatibility and crystallization behaviors of chemically bonded PA 6/PTFE compounds were investigated by means of wide-angle X-ray diffraction (WAXD), DSC, and DMTA [12]. WAXD measurements showed that no co-crystallization occurred between two components, while DSC and DMTA measurements suggested that a certain degree of compatibility between them might exist due to the formation of some copolymers during the reactive extrusion. In the present paper, the α transition of PA 6 component in these compounds will be further studied by combining DMTA and DETA to elucidate the effect of PTFE component on the molecular dynamics of PA 6.

Experimental part

Materials

The parent homopolymers, both PA 6 and PTFE were commercial grades. PA 6-SH 6 pellets were supplied by Leuna A.G., Germany, and PTFE-MP 1100 powders were supplied by Dupont Corp., Del., USA. Chemically bonded PA 6/PTFE compounds were prepared by reactive extrusion and supplied kindly by Dr. D. Lehmann of Institute for Polymer Research, Dresden, Germany. The details about the preparation process could be found elsewhere [1, 2]. As-received PA 6/PTFE samples were pressed under a pressure of ca. 25 GPa at ca. 448 K (175 °C) (ca. 46 K below the melting temperature (T_m) of PA 6 component of ca. 494 K (221 °C) measured by DSC at 10 K min^{-1}) for ca. 5 min to form thin films with a thickness of ca. 0.5 mm. Only at so low temperature, could the obtained thin films have smooth surface which is essential to the subsequent DMTA and DETA measurements. Then they were cooled at ca. 5 K min^{-1} to the ambient temperature of ca. 298 K. Subsequently, prepared thin films were cut into equal rectangles with a size of ca. 25.0 × 5.0 mm^2 (for DMTA measurements) or circles with a diameter of ca. 30.0 mm (for DETA measurements).

DMTA and DETA measurements

DMTA measurements were performed in a Rheometric Scientific DMTA V at a frequency of 1 Hz and a heating rate of 5 K min^{-1}. A tension mode was employed. DETA measurements were performed in a TA 2970 DETA. The samples were sandwiched between the ceramic parallel plate sensors with a diameter of ca. 25.0 mm and a maximum compression force of ca. 300 N was exerted to ensure good contact between the samples and the electrodes. A frequency range from 2×10^{-2} to 10^5 Hz and a heating rate of 2 K min^{-1} were employed. In both DMTA and DETA measurements, a dry nitrogen gas purge with a flux of ca. 500 mL min^{-1} was used to prevent oxidative degradation of samples during the heating run.

DSC measurements

The T_m and the degree of crystallinity (X_c) of PA 6 and PTFE components were measured by using a TA 2910 DSC. Indium and tin were employed for the temperature calibration, and the specific heat capacity was evaluated with respect to sapphire as a standard. The samples with a mass of ca. 5.0 mg were cut from the prepared thin films and sealed in aluminum pans. A dry nitrogen gas purge with a flux of ca. 20 mL min^{-1} was used to prevent oxidative degradation of samples during the heating run. The heating rate in DSC was 20 K min^{-1}. Only a single well-defined endothermic melting peak without corresponding exothermic cold crystallization peak was found for each component in the DSC traces of the first heating run. Therefore, X_c can be calculated as follows [13],

$$X_c(\%) = \frac{\Delta H_m}{\Delta H_m^0} \cdot 100 \quad (1)$$

where ΔH_m was the melting enthalpy of PA 6 or PTFE component, and ΔH_m^0 was the melting enthalpy of its perfect crystalline lamellae. For PA 6 and PTFE components, their ΔH_m^0's were 230.1 and 92.8 J g^{-1}, respectively [14, 15]. It should be mentioned that ΔH_m had been normalized by the weight fraction of each component in the compounds.

Results and discussion

Figure 1 presents DMTA loss tangent (tan δ) curves for PA 6/PTFE compounds with various compositions. It can be seen that there was a peak appearing in the temperature range of ca. 333–338 K (60–65 °C), which corresponds to the α transition of PA 6 component associated with the glass transition. It also can be seen that with the increase of weight fraction of PTFE component (w^{PTFE}), the peak shifted slowly to lower temperatures, and the peak value (tan δ_{max}) decreased slightly.

Figure 2 presents DETA tan δ curves for the same samples as shown in Fig. 1. It can be seen that there was also a peak appearing in the temperature range of ca. 350–359 K (77–86 °C), which also corresponds to the α transition of PA 6 component. It should be noted that at higher temperatures, tan δ increased sharply due to the contribution of the ionic conductance together with the interfacial

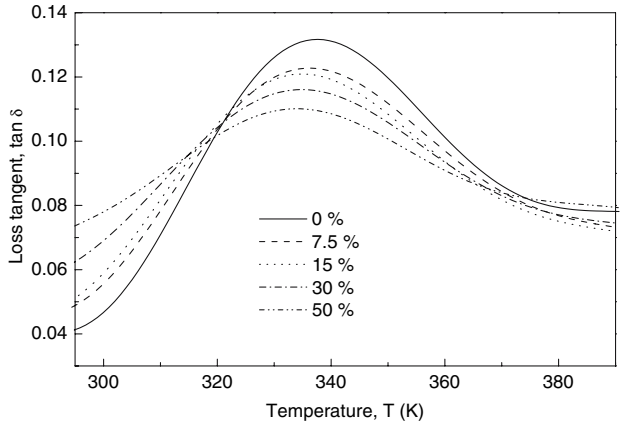

Fig. 1 DMTA tan δ curves at 1 Hz for PA 6/PTFE compounds with various weight percentage of PTFE component indicated in the corner

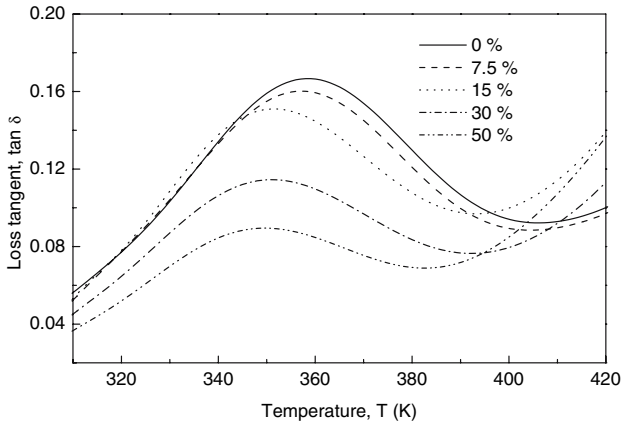

Fig. 2 DETA tan δ curves at 10^5 Hz for PA 6/PTFE compounds with various weight percentage of PTFE component indicated in the corner

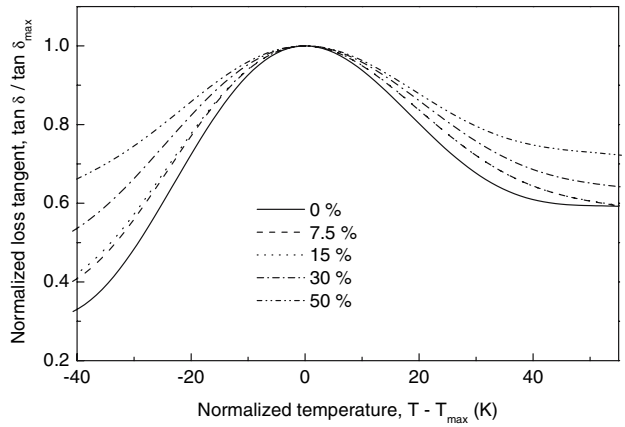

Fig. 3 Normalized DMTA tan δ curves at 1 Hz for PA 6/PTFE compounds with various weight percentage of PTFE component indicated in the corner (obtained from Fig. 1)

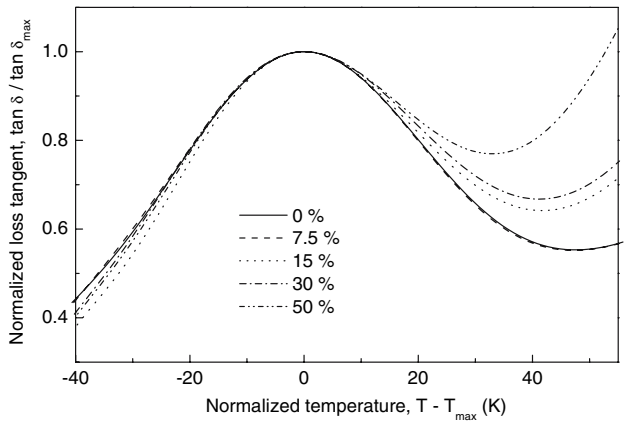

Fig. 4 Normalized DETA tan δ curves at 10^5 Hz for PA 6/PTFE compounds with various weight percentage of PTFE component indicated in the corner (obtained from Fig. 2)

polarization originated from polar PA 6/non-polar PTFE interface [16]. It also can be seen that with the increase of w^{PTFE}, the peak shifted to lower temperatures, and the tan δ_{max} decreased greatly.

Figures 3 and 4 present the normalized curves of tan δ/tan δ_{max} versus T–T_{max} for the α transition of PA 6 component obtained from Figs. 1 and 2, respectively, where tan δ represents the value of loss tangent at any temperature T and tan δ_{max} represents the loss tangent value at the corresponding T_{max} temperature. The width of these normalized curves indicates the heterogeneity of phase and thus the compatibility of PA 6 component with PTFE component in the compounds [16, 17]. A great difference can be found between Figs. 3 and 4. As shown in Fig. 3, the increase of w^{PTFE} resulted in a remarkable broadening of the normalized curves for the α transition of PA 6 component, which implies the wider distribution of the segmental mobility, while Fig. 4 does not present any obvious change with the increase of w^{PTFE} except the high temperature side which was caused by the ionic conductance together with the interfacial polarization as mentioned above [16]. Clearly, Fig. 3 suggests good compatibility between PA 6 and PTFE components while Fig. 4 seems to imply poor compatibility between them. This great difference must be understood by considering the different mechanisms between DMTA and DETA as mentioned above [9, 10].

Figure 5 presents the evolution laws of tan δ_{max} with the increase of w^{PTFE} for PA 6/PTFE compounds measured by both DMTA and DETA at various frequencies and heating rates. It can be seen that for each group of six measurement points the left five data followed good linearity, which suggests homogeneous dispersion of PTFE component in the continuous phase of PA 6 component. By extrapolating w^{PTFE} to the value of 100%, it can be seen that tan δ_{max} reached almost zero for DETA measurements at both frequencies of 10^4 and 10^5 Hz, while had a value of ca. 0.089 for DMTA measurements at 1 Hz. It suggests that PTFE

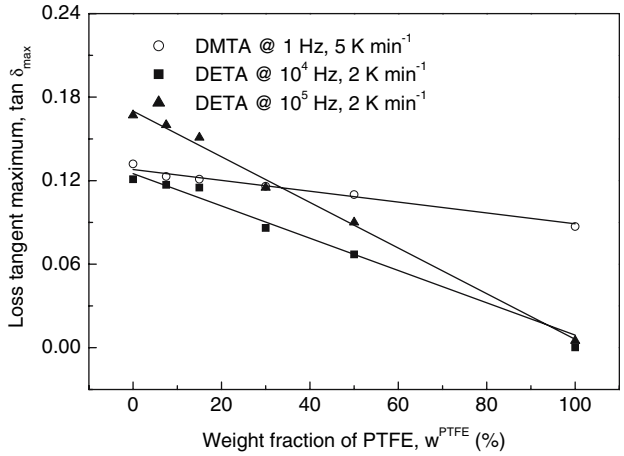

Fig. 5 Evolution of tan δ_{max} with increasing w^{PTFE} for PA 6/PTFE compounds measured by both DMTA and DETA at various frequencies and heating rates indicated in the corner. The solid lines are linear fits to the left five points for each group of six measurement points

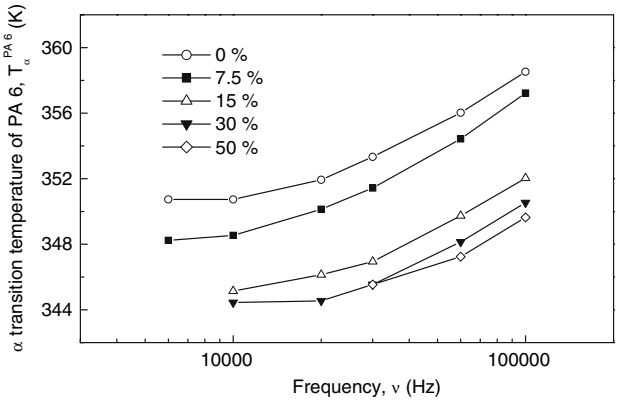

Fig. 6 Evolution of $T_\alpha^{PA\ 6}$ with increasing ν for PA 6/PTFE compounds with various weight percentage of PTFE component indicated in the corner

component contributed to the tan δ_{max} measured by DMTA at the T_{max} of PA 6 component ($T_\alpha^{PA\ 6}$) while barely did to the tan δ_{max} measured by DETA. The rightmost point is the value for pure PTFE measured at the temperature, where the evolution laws of $T_\alpha^{PA\ 6}$ with increasing w^{PTFE} had been considered. It can be seen that for all three groups of data, the measured point was in excellent agreement with the value obtained by extrapolating the linear fits. According to these results, it is clear that at $T_\alpha^{PA\ 6}$, the dynamic mechanical response of PTFE component was remarkable while its dielectric response was negligible. Between these two interesting findings, the former can be easily understood, while the latter should be explained on the basis of the non-polar character of PTFE component [18–20]. That is to say, PTFE component was dielectrically inactive at the temperature of $T_\alpha^{PA\ 6}$ due to its non-polarity.

Figure 6 presents the evolution laws of $T_\alpha^{PA\ 6}$ with increasing frequency (ν) measured from DETA tan δ curves. It should be noted that in our experiments $T_\alpha^{PA\ 6}$ could only be detected at high ν. For example, $T_\alpha^{PA\ 6}$ of the pure PA 6 samples could be obtained only at ν above a critical value (ν_c) of 6×10^3 Hz. This is due to the fact that at low ν, the disturbance of the ionic conductance together with the interfacial polarization masked the tan δ peak [16]. From Fig. 6, it can be seen that $T_\alpha^{PA\ 6}$ increased with either the increase of ν or the decrease of w^{PTFE}. Between these two evolution laws, the former is a common phenomenon while some interesting information can be obtained from the latter. According to the evolution laws of $T_\alpha^{PA\ 6}$ with the change of w^{PTFE}, it is clear that the segmental mobility of PA 6 component was increased by the PTFE component in PA 6/PTFE compounds and this effect enhanced greatly with the increase of w^{PTFE}.

Table 1 presents the T_m and X_c of PA 6 and PTFE components in the compounds measured by DSC. With the increase of w^{PTFE}, no definite change could be seen for the T_m of PTFE component, a slight decrease was found for both the T_m and the X_c of PA 6 component, and a significant increase occurred for the X_c of PTFE component. Obviously, coupled with the addition of PTFE component, both the perfection and the amount of PA 6 crystallites decreased slightly, the amount of PTFE crystallites increased remarkably, however, the perfection of PTFE crystallites kept almost the same due to its excellent crystallizability. In order to make our analysis more convenient, also taking into account of the high crystallizabiltiy of PTFE, semicrystalline PTFE component can be seen as a dual-phase system and the interphase between crystallites and amorphous phase is not involved [21–23]. According to this assumption, weight fraction of the amorphous phase of PTFE component (w_a^{PTFE}) can be estimated as follows,

$$w_a^{PTFE} = w^{PTFE}(1 - X_c^{PTFE}) \quad (2)$$

Table 1 T_m and X_c of PA 6 and PTFE components in PA 6/PTFE compounds measured by DSC at 20 K min^{-1} (the value of w_a^{PTFE} is also included as the rightmost column)

w^{PTFE} (%)	T_m (K)		X_c (%)		w_a^{PTFE} (%)
	PA 6	PTFE	PA 6	PTFE	
0	494.0	–	26.8	–	–
7.5	494.5	594.7	26.9	39.1	4.6
15	494.2	594.5	26.4	48.1	7.8
30	494.2	594.5	26.8	51.8	14.5
50	493.6	594.8	25.6	57.3	21.4
100	–	594.9	–	61.7	38.3

where X_c^{PTFE} is the X_c of PTFE component. As shown in Table 1, coupled with the rapid increase of X_c^{PTFE}, w_a^{PTFE} also increased with the increase of w^{PTFE}. However, we cannot draw a conclusion that the dilution effect of PTFE component caused by simple blending played a dominant role in the increasing segmental mobility of PA 6 component as shown in Fig. 6 after considering the extreme incompatibility between PA 6 and PTFE homopolymers [1, 2]. Therefore, it seems plausible to conclude that the chemical bonding effect plays the dominant role.

As a matter of fact, PA 6 and PTFE have poor compatibility because of their extremely different polarity and surface energy [1, 2]. When these two components had been chemically bonded during the reactive extrusion, their compatibility would be enhanced greatly due to the formation of PA 6/PTFE graft and block copolymers [1, 2]. This effect has been shown clearly in Fig. 3 where the broadening of normalized DMTA tan δ curves was remarkable. However, no experimental evidence was given by DETA measurements due to the different mechanisms of DETA as mentioned above [9, 10].

Vogel–Fulcher equation is often employed to express the molecular dynamics of polymers near the α transition as follows [24, 25],

$$v = A \cdot \exp\left[\frac{-\Delta E_a}{R(T - T_0)}\right] \quad (3)$$

where T is the T_α at any frequency v, A is the pre-exponential factor, ΔE_a is the apparent activation energy, R is the universal gas constant, and T_0 is the reference temperature. Such fits have been done for all the samples as shown in Fig. 7 and obtained parameters are shown in Table 2. From Table 2, it can be seen that A kept almost

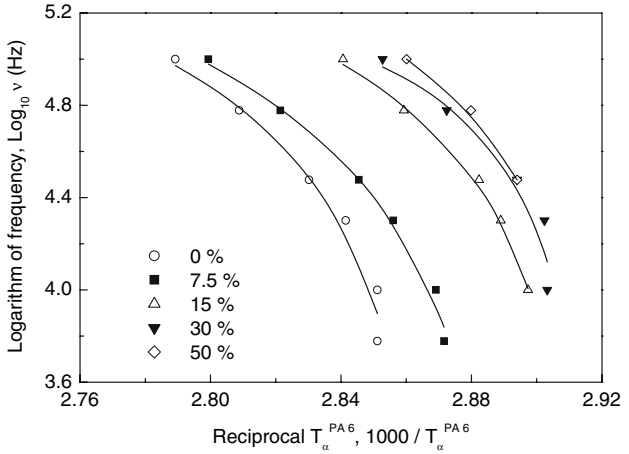

Fig. 7 Arrhenius plots of Log_{10} v versus $1{,}000/T_\alpha^{PA\ 6}$ for PA 6/PTFE compounds with various weight percentage of PTFE component indicated in the corner. The solid lines are fits to the Vogel–Fulcher equation [24, 25]

Table 2 Vogel–Fulcher parameters for the α transition of PA 6 component in PA 6/PTFE compounds

w^{PTFE} (%)	T_0 (K)	ΔE_a (kJ mol^{-1})	Log_{10} A	Relativity
0	346.0	156.6	5.626	0.98556
7.5	342.1	225.5	5.757	0.99514
15	340.6	140.3	5.618	0.99819
30	341.8	61.4	5.333	0.96981
50	341.0	96.0	5.581	1.00000

constant and T_0 decreased slightly with the increase of w^{PTFE}. It also can be seen that ΔE_a decreased with the increase of w^{PTFE}, which suggests that the addition of PTFE component reduced the cooperativity of the α transition of PA 6 component [26].

Conclusion

α Transition of PA 6 in chemically bonded PA 6/PTFE compounds was studied by combining DMTA and DETA to elucidate the effect of PTFE component on the molecular dynamics of PA 6 component. It was found that DMTA showed good compatibility between these two components, while DETA did not give any experimental evidence. It was also found that at the temperature of $T_\alpha^{PA\ 6}$, the dynamic mechanical response of PTFE component was remarkable while its dielectric response was negligible. The effect of PTFE on the segmental mobility of PA 6 component was discussed by DMTA, DETA and DSC results, and the chemical bonding effect was found to play the dominant role. The measurement of ΔE_a showed that the addition of PTFE component reduced the cooperativity of the α transition of PA 6 component.

Acknowledgements The financial support from the Joint Program between Max Planck Society (MPG) and Chinese Academy of Sciences (CAS) is appreciated. The author would also like to thank Dr. D. Lehmann (Institute for Polymer Research, Dresden, Germany) for providing the samples.

References

1. Hupfer B, Lehmann D, Reinhardt G, Lappan U, Geissler U, Lunkwitz K, Kunze K (2001) Kunstst Plast Eur 91:50
2. Lehmann D, Hupfer B, Lappan U, Pompe G, Haussler L, Jehnichen D, Janke A, Geissler U, Reinhardt R, Lunkwitz K, Franke R, Kunze K (2002) Des Monomers Polym 5:317
3. Eichhorn KJ, Lehmann D, Voigt D (1996) J Appl Polym Sci 62:2053
4. Haeussler L, Pompe G, Lehmann D, Lappan U (2001) Macromol Symp 164:411
5. Pompe G, Haeussler L, Poetschke P, Voigt D, Janke A, Geissler U, Hupfer B, Reinhardt G, Lehmann D (2005) J Appl Polym Sci 98:1308

6. Pompe G, Haeussler L, Adam G, Eichhorn K-J, Janke A, Hupfer B, Lehmann D (2005) J Appl Polym Sci 98:1317
7. Factor BJ, Mopsik FI, Han CC (1996) Macromolecules 29:2318
8. Canadas JC, Diego JA, Sellares J, Mudarra M, Belana J, Diaz-Calleja R, Sanchis MJ (2000) Polymer 41:2899
9. Hardy L, Stevenson I, Boiteux G, Seytre G, Schonhals A (2001) Polymer 42:5679
10. Vatalis AS, Kanapitsas A, Delides CG, Viras K, Pissis P (2001) J Appl Polym Sci 80:1071
11. Zhao J, Wang J, Li C, Fan Q (2002) Macromolecules 35:3097
12. Song R, Zhao J, Stamm M (2004) Macromol Mater Eng 289:1053
13. Dong W, Zhao J, Li C, Guo M, Zhao D, Fan Q (2002) Polym Bull (Berlin) 49:197
14. van Krevelen DW (2003) Properties of polymers, their correlation with chemical structure; their numerical estimation and prediction from additive group contributions, 3rd completely revised edn. Elsevier, Amsterdam
15. Starkweather HW, Zoller JP, Jones GA, Vega AJ (1982) J Polym Sci Polym Phys 20:751
16. Leyva ME, Soares BG, Khastgir D (2002) Polymer 43:7505
17. Zetsche A, Kremer F, Jung W, Schulze H (1990) Polymer 31:1883
18. Starkweather HW, Avakian P, Matheson RR, Fontanella JJ, Wintersgill MC (1991) Macromolecules 24:3853
19. Starkweather HW, Avakian P, Matheson RR, Fontanella JJ, Wintersgill MC (1992) Macromolecules 25:1475
20. Starkweather HW, Avakian P, Fontanella JJ, Wintersgill MC (1994) Macromolecules 27:610
21. Boyer RF (1973) Macromolecules 6:288
22. Boyer RF (1973) J Macromol Sci Phys B8:503
23. Struik LCE (1987) Polymer 28:1521, 1534; (1989) 30:799, 815
24. Vogel H (1921) Phys Z 22:645
25. Fulcher GS (1925) J Am Ceram Soc 8:339
26. Starkweather HW (1993) Macromolecules 26:4805